Hydrographic characterization of southeast Arabian Sea during the wane of southwest monsoon and spring intermonsoon

ARTICLE *in* ENVIRONMENTAL MONITORING AND ASSESSMENT · MAY 2008

Impact Factor: 1.68 · DOI: 10.1007/s10661-007-9863-3 · Source: PubMed

8 AUTHORS, INCLUDING:


Smitha BR
Centre For Marine Living Resources and Ecology
12 PUBLICATIONS **49** CITATIONS


Habeebrehman H
Farook College
9 PUBLICATIONS **96** CITATIONS


K.R. Muraleedharan
National Institute of Oceanography
31 PUBLICATIONS **161** CITATIONS


V. N. Sanjeevan
Centre For Marine Living Resources and Ecology
51 PUBLICATIONS **137** CITATIONS

Environ Monit Assess
DOI 10.1007/s10661-007-9863-3

Hydrographic characterization of southeast Arabian Sea during the wane of southwest monsoon and spring intermonsoon

K. G. Vimal Kumar · P. K. Dinesh Kumar · B. R. Smitha · H. Habeeb Rahman · Jacob Josia · K. R. Muraleedharan · V. N. Sanjeevan · C. T. Achuthankutty

Received: 30 September 2006 / Accepted: 3 July 2007

Abstract Seasonal variation of the hydrography along the southeast Arabian Sea is described using data collected onboard FORV Sagar Sampada in September–October 2003 (later phase of Southwest monsoon, SWM) and March–April 2004 (Spring inter monsoon, SIM). During the later phase of the SWM, upwelling was in the withdrawal phase and the frontal structure was clearer in the northern sections (13 and 15°N lat) indicating strong upwelling in the area. The driving force of upwelling is identified as the combination of alongshore wind stress and remote forcing with a latitudinal variability. Although a more prominent upwelling was found in the north, a maximum surface Chlorophyll-*a* was found in the south (10°N). During the SIM, the area was characterized by oligotrophic water with relatively high Sea Surface Temperature (>29°C) and low salinity (33.8 to 35.4). During March, the surface hydrography was found to be controlled mainly by the intrusion of low-saline waters from the south, while during September by the high saline water from the north. The presence of various water masses [Arabian Sea High Salinity Water (ASHSW), Persian Gulf Water (PGW), Red Sea Water (RSW)] and their seasonal variations in the region is discussed and their decreasing influence towards the south is noted during both periods of observation. During the SWM, the dynamic topography showed the equator-ward flow of the West India Coastal Current (WICC) at the surface and a pole-ward coastal under current at sub-thermocline depth. During the SIM, surface circulation revealed the WICC flowing pole-ward north of 13°N, but equator-ward flow in the south, with a clockwise circulation around the Lakshadweep High.

Keywords Upwelling · Arabian Sea high salinity water · Pole-ward undercurrent · Arabian Sea · Hydrography

K. G. Vimal Kumar · P. K. Dinesh Kumar (✉) · B. R. Smitha · H. Habeeb Rahman · J. Josia · K. R. Muraleedharan · C. T. Achuthankutty
Regional Centre, National Institute of Oceanography, P.O. Box 1913, Kochi 682018, Kerala, India
e-mail: dineshku@nio.org

V. N. Sanjeevan
Centre for Marine Living Resources and Ecology, Ministry of Earth Sciences, Kochi 682037, Kerala, India

Introduction

The Arabian Sea (AS), situated in the northwestern part of the Indian Ocean, is bounded by the Asian land mass and Africa to the north and west and by the Indian subcontinent to the east. The AS is distinct from the other low-latitude seas by being semi-enclosed and under the influence of monsoonal winds, which reverse their direction and give rise to two distinct seasons i.e., Southwest (Summer, SWM) and Northeast (Winter, NEM) Monsoon. Associated with seasonal changes of the wind field, surface circulation of the system also reverses thoroughly.

Some of the earlier studies on the hydrography of the southeastern Arabian Sea (SEAS) such as, Sastry and Myrland (1959), Ramamirtham and Jayaraman (1960), Jayaraman et al. (1960), and Patil and Ramamirtham (1963). Rochford (1964), Wyrtki (1971), Varadachari et al. (1974) specifically described the different water mass formed in the Arabian Sea. Shetye et al. (1990, 1991) provided general information on the hydrography and circulation of the SWM and NEM along the west coast of India. Prasanna Kumar and Prasad (1999) gave an account of the formation and seasonal spreading of Arabian Sea High Salinity Water (ASHSW) towards the southern Arabian Sea. Banse (1959), Darbyshire (1967), Sharma (1978), Johannessen et al. (1981), Muraleedharan and Prasanna Kumar (1996) described phenomena of upwelling during the SWM along the South West coast. Using in situ data Shetye et al. (1990) established the presence of the West India Coastal Current (WICC) on the surface and pole-ward under current during the SWM. Antony (1990) inferred the presence of under current at 15°N, and Muraleedharan et al. (1995) studied the under current using in situ data during both monsoon and non-monsoon seasons between 8 and 15°N. During spring Inter Monsoon (SIM) the SEAS experience high SST (>29°C) and Joseph (1990) called this the Indian Ocean warm pool because it is the warmest area of the world oceans during March–May months. The down-welling and low salinity surface water provided conditions for the formation of high SST during SIM (Shenoi et al. 1999). Shenoi et al. (2005) inferred the circulation pattern based on the spatial patterns of salinity during SIM. Moreover, the model results of Joseph and Kantha (2000) indicate that SEAS is a region of higher variability than the northern eastern Arabian Sea because it is a location of Laccadive High and other eddies generated during NEM (Bruce et al. 1994). Using the most recent data sets available, the present study tries to bring together the features of hydrography and current structure during transition period i.e. the last phase of the SWM and the spring inter monsoon (SIM) periods.

Materials and methods

In connection with the Marine Living Resources programme of the Department of Ocean Development (Ministry of Earth Sciences), Govt. of India, hydrographic surveys were carried out on board FORV Sagar Sampada in September–October 2003 (SS-217) in the SEAS. The stations were repeated during March–April 2004 (SS-223) to study the seasonal variation (Fig. 1). Data on surface winds was collected by the automated weather station at 1 min intervals on board the ship (with accuracy of ± 0.3 m/s and ± 3° for wind speed and direction respectively). A Sea Bird CTD (accuracy of conductivity 0.0003 S/m, temperature 0.001°C, and Pressure 0.015%) was operated along five sections (8, 10, 11.3, 13 and 15° N) up to 1,000 m. CTD-derived salinities were calibrated against those from the samples collected simultaneously with a rosette sampler and analyzed with Guildline 8400 Autosal.

Hydrographic properties changed mostly in the upper 200 m. Horizontal and vertical sections of temperature and salinity up to 200 m were prepared as aids to understand the water characteristics. The dynamic topography with reference to 500 db was studied to understand the circulation pattern. The anomaly of the dynamic depth (ΔD) is given by $\Delta D = {}_0\int^P \delta \, dP$, where δ is the specific volume anomaly and P is the pressure in decibars.

Upwelling can be characterized by two indices: the local temperature anomaly (LTA) and the offshore-Ekman transport (M_x). The LTA is obtained by subtracting the temperature of the near coastal station from that at the outer most station. The offshore Ekman transport M_x (kg m^{-1} s^{-1}), computed from $M_x = \tau_y / f$, τ_y, is the along shore wind stress (dyne/cm^2) and f = 2Ωsinϕ is the Coriolis force. The along shore wind stress τ (dyne/cm^2) was computed from the bulk-aero dynamic formulae $\tau = \rho_a C_d v^2$ where ρ_a is the air density, v is the wind speed (m/s) and C_d is the dimensionless drag coefficient (a constant value of 1.3×10^{-3} is considered, which has been found

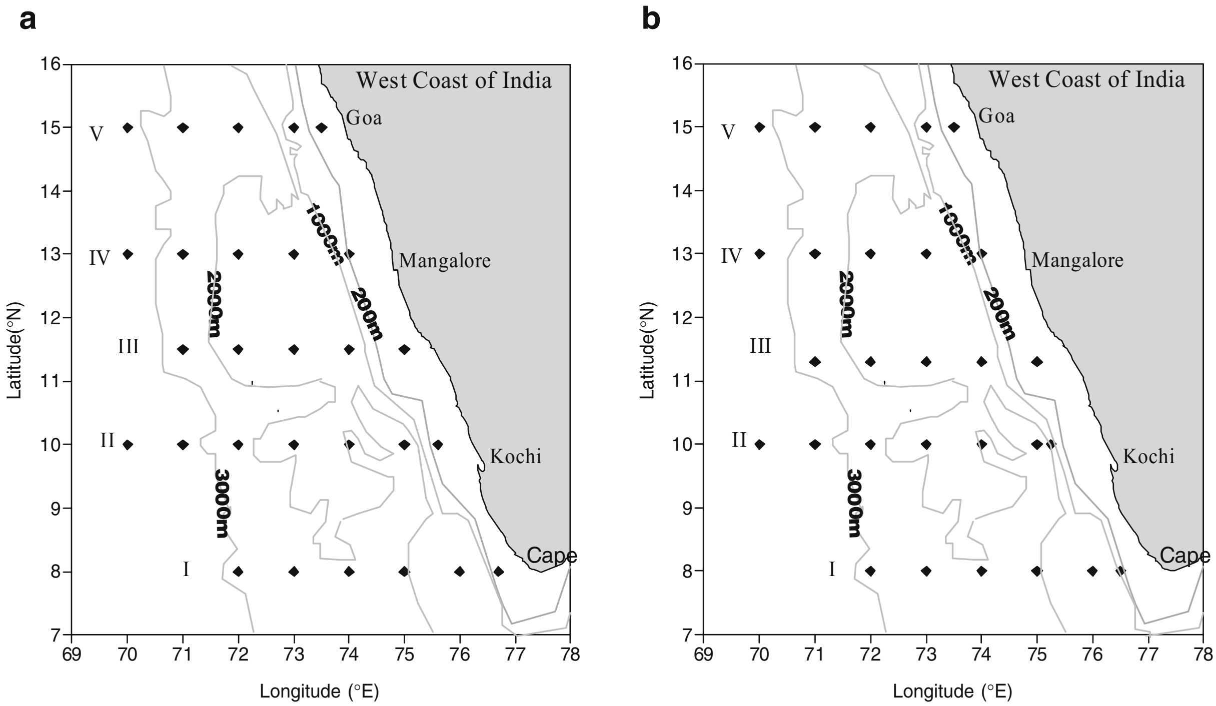

Fig. 1 Station locations during **a** 13th September – 5th October, 2003 and **b** 18th March – 8th April, 2006

appropriate in earlier investigations of coastal regions (Prell and Streeter 1982; Shetye et al. 1985).

Water samples from standard depths (0, 10, 20, 30, 50, 75, 100 and 150) were analysed for nitrate and phosphate with a SKALAR auto analyzer and dissolved oxygen was estimated using Winkler's method. The Chlorophyll *a* (chl *a*) was determined by filtering 1 l from the seven standard depth (surface to 120 m) through 47 mm GF/F filters (nominal pore size 0.7 μm) under low vacuum (less than 100 mmHg). The filters were deep frozen immediately. In the shore laboratory, chl a. was extracted in 10 ml of 90% acetone in the dark for 24 h in a refrigerator and estimated (Strickland and Parsons 1972) with a spectrophotometer (Perkin-Elmer UV/Vis). Vertical distribution of dissolved oxygen, nutrients and chlorophyll were considered for near shore stations only because upwelling occurs close to the shelf area.

The SeaWiFS monthly climatology data used for the present study is downloaded from the ocean color ftp site. The current climatology data are derived by time-binning the monthly-binned files from September 1997 to August 2004 and mapping to an Equidistant Cylindrical projection, with 9 km resolution at the equator.

Results

Hydrographic characteristics during the later phase of south west monsoon

Low SST was recorded along the coast and high SST observed offshore. The highest LTA between the coastal and offshore stations was observed along 15°N (2°C) and the lowest (0.2°C) at southernmost transect (8°N). In general, decrease in temperature from offshore to coast and from south to north was observed (Fig. 2a). The surface salinity was characterized by low values (34.4–34.9) on the shelf and high salinities (>36.2) farther offshore. The sigma-t structure resembled that of temperature, indicating that the surface distribution of sigma-t depended more on temperature than on salinity.

The vertical distributions of temperature, salinity and density to 200 m depth, along the five transects

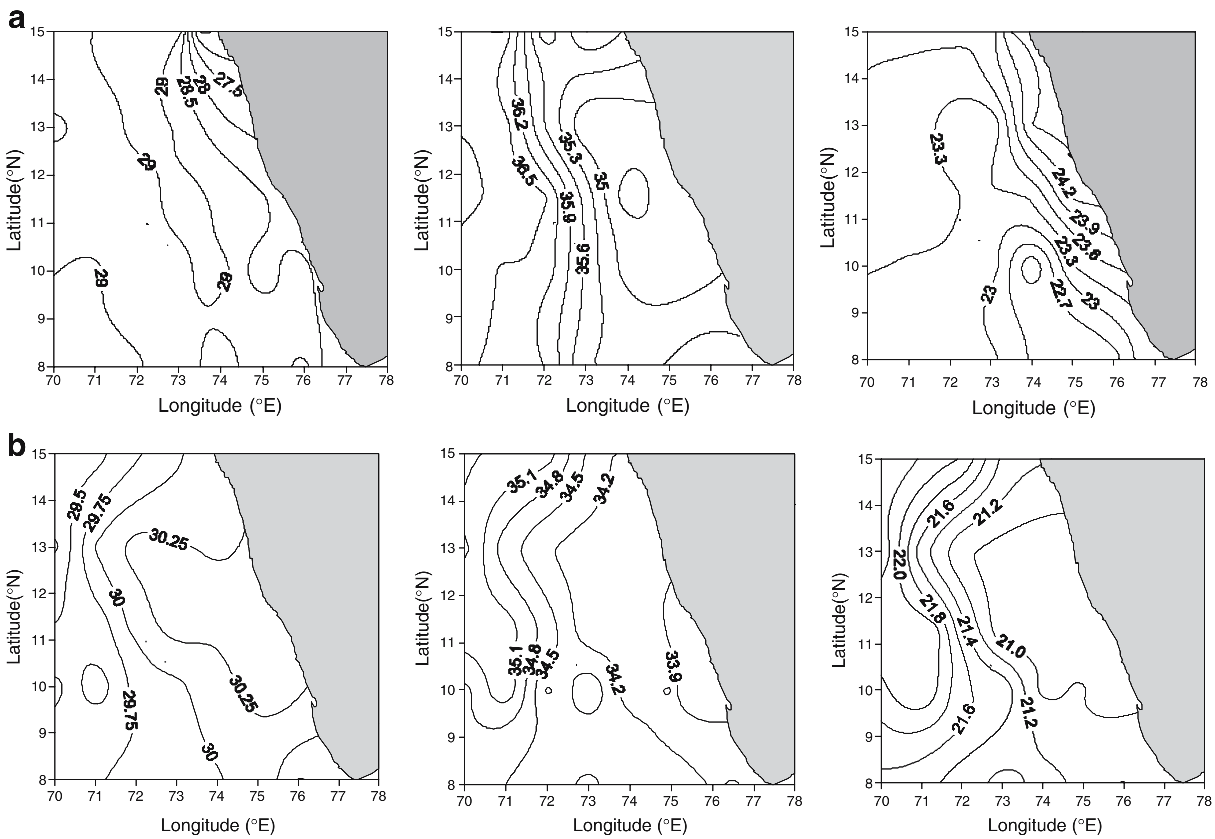

Fig. 2 Surface distribution of temperature (°C), salinity and density during **a** later phase of southwest monsoon and **b** spring intermonsoon

(I–V) are shown in Figs. 3a, 4a, 5a, 6a and 7a. At all the five sections, the upsloping of isolines from 80 to 100 m to the surface layer on the shelf was a conspicuous feature in September, causing a considerable fall of surface temperature indicative of coastal upwelling. The thickness of the thermocline gradually decreased from north to south. A temperature gradient of 0.08 to 0.1°C/m was noted in the thermocline. Another feature found at all five sections was the bending down of deeper isotherms and isopycnals below the upwelled water at the nearest coastal station.

The high-salinity offshore water present at the surface on all sections and extending from 50 to almost 100 m depth was subducted below the low-salinity surface layer at mid-longitudes at and north of section III. The intermediate salinity maximum so formed reached the coastal station only in section V, but the vertical density gradient was greatly altered. Shelf waters of the sections I to IV displayed a difference of 0.7 horizontally and of 0.8 downward to 150 m depth. But the northernmost section V, showed high vertical difference in salinity (2) due to the intrusion of high saline water into the shelf waters in the surface layer. Vertical section of the slope water showed that the core was limited to a layer between 50 and 80 m. In general, high saline water hugging the shelf area was found to get dissipated towards southern transects.

The sigma-t distributions along the sections depict high stratification in the upper layers of the continental shelf, whereas stratification was weak offshore. Upsloping of isopycnals indicates upwelling. Downsloping of isopycnals was noted between 100 and 200 m towards slope/shelf break area. One unique feature observed was the maximum sigma-t gradient (2.2 to 3.0 kg/m^3) in the upper 50 m of the shelf indicating strong onshore flow.

Low oxygenated and nutrient rich waters characterized the shelf water along the southwest coast of

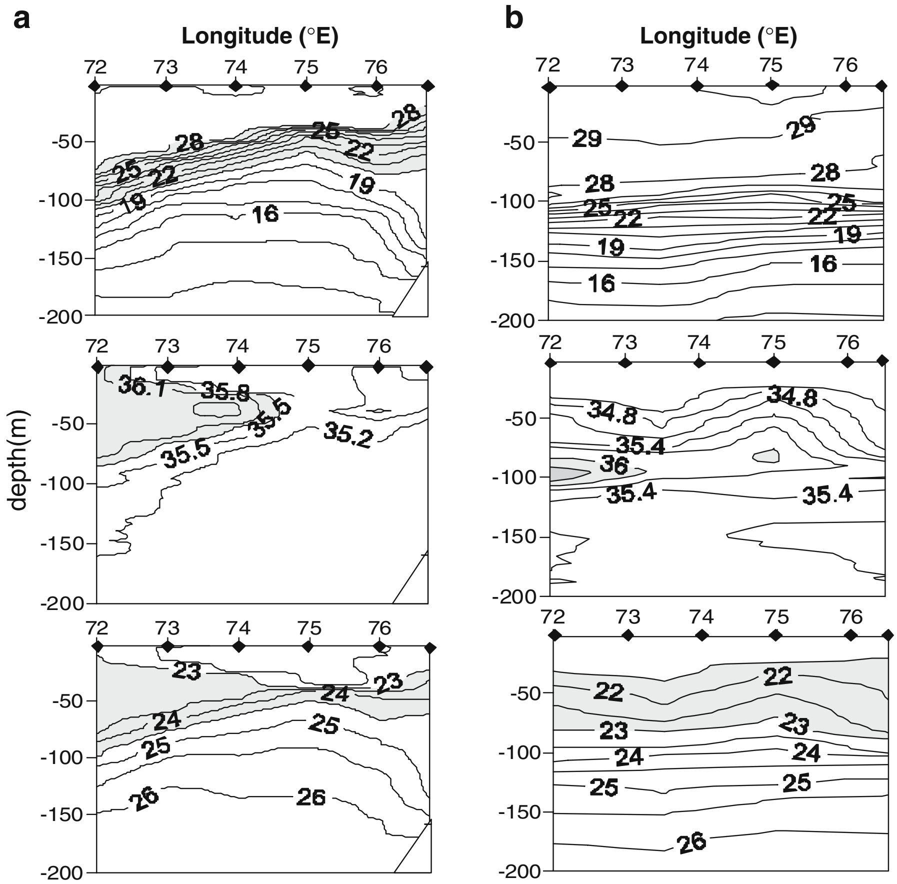

Fig. 3 Vertical distribution of temperature (°C), salinity and density (σ_t) along 8°N during **a** later phase of Southwest monsoon and **b** spring intermonsoon. *Shaded profiles* represent upslope/downslope in temperature and density sections, intrusion of high salinity water in the salinity section

India during the later phase of SWM (Fig. 8a). The upwelling signatures prevalent in the southern region might have subsided, since this period is the late phase of summer monsoon. But upwelling signatures were still observed along the 10, 11.5, 13 and 15°N transects even during the later phases of summer monsoon, which is evident from the upsloping of the isolines of 190 μM of DO, 2 μM of nitrate and 1 μM of phosphate to the surface along these latitudes. Intense upwelling was observed along 13–15°N transects as evidenced by the surfacing of the 0.8 and 190 μM isolines of phosphate and dissolved oxygen. This indicates the prevalence and dominance of upwelling signatures towards the northern transects (13–15°N) during late summer with indications of receding of upwelling signatures from the southernmost transects (8–10°N).

The distribution of chlorophyll-*a* (chl-*a*) showed that surface chl-*a* ranged from 0.1 to 0.75 mg m^{-3} (av. 0.24 mg m^{-3}) and the integrated value of chl-*a* in the euphotic column (up to 120 m) was between 15 and 60.7 mg m^{-2} (av. 33.8 mg m^{-2}) in the near-shore stations during the later phase of Summer monsoon (Fig. 9). Latitudinal variations in the chl-*a* distribution showed that the surface maximum was observed off Kochi and off Mangalore and the lowest value was found along 15°N.

To understand the flow characteristics of the area, the dynamic topography for surface (3 db), 50, 100 and 200 db relative to 500 db is presented in Fig. 10. (Since the readings of the initial few meters of some stations were not reliable, data at 3 db were considered as the surface level). During the cruise, the surface circulation between 8 and 15°N was characterized by an organized equator-ward flow on the shelf except south of 10°N on the shelf and above the continental slope where the flow was to the north. Between 15 and 11°N near the coast, southward flow was broad but it narrowed towards the southern transects. At the 50 db level, the flow was the same as near the surface, but less strong. The topography at

Fig. 4 Vertical distribution of temperature (°C), salinity and density σ_t along 10°N during **a** later phase of Southwest monsoon and **b** spring intermonsoon. *Shaded profiles* represent upslope/downslope in temperature and density section, intrusion of high salinity water in the salinity section

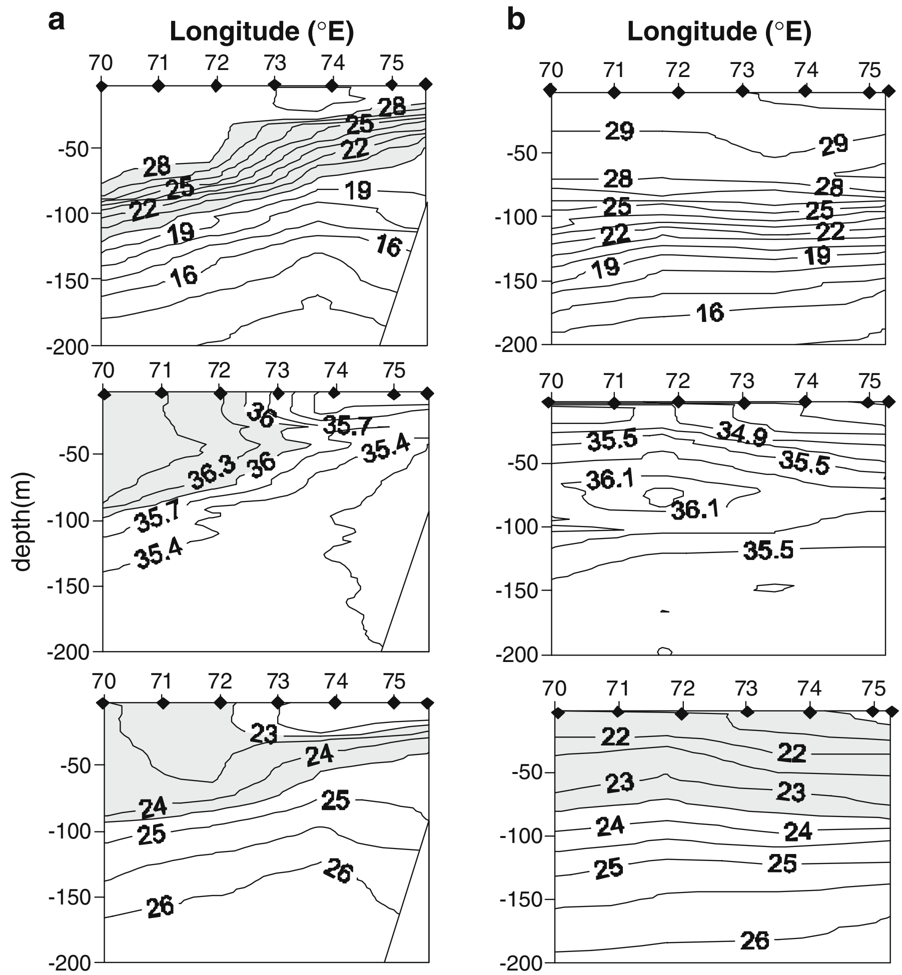

100 db indicated northerly flow on the shelf and equator-ward flow off the shelf. At 200 db, the same circulation pattern was observed but with reduced strengths.

Hydrographic characteristics during the spring inter monsoon

The SST was 29.5 to 30.3°C with small horizontal differences (Fig. 2b). The general trend of SST was a decrease inshore towards offshore regions. The surface salinity near-shore ranged from 33.8 to 34.2 and offshore from 34.6 to 35.2. In general, the horizontal gradient between shelf and offshore waters was about 1.4 but with an approximately north-south front between 71 and 73°E. The surface density reflected salinity distribution.

The vertical distribution of temperature (Figs. 3b, 4b, 5b, 6b and 7b) indicated a warm weakly stratified surface layer up to 60 m (80 m at 8°N) along 1 to V sections. The top of the thermocline generally occurred at 90 to 100 m depth. Below 100 m, the upward lift of isotherms indicated the equator ward under currents along the shelf waters (at sections III, IV and V) of the study area. Upsloping of isotherms along section I indicates the signature of initial stage of upwelling in the southern most transect; and nearest coastal station of all other sections displayed downward bending of isotherms.

Except the upper 20–30 m on section I (8°N), the layer above the thermocline was stratified by low salinity along all transects, the water having been advected from the Bay of Bengal. Below, roughly 50 to 100 m, there was a layer of markedly increased

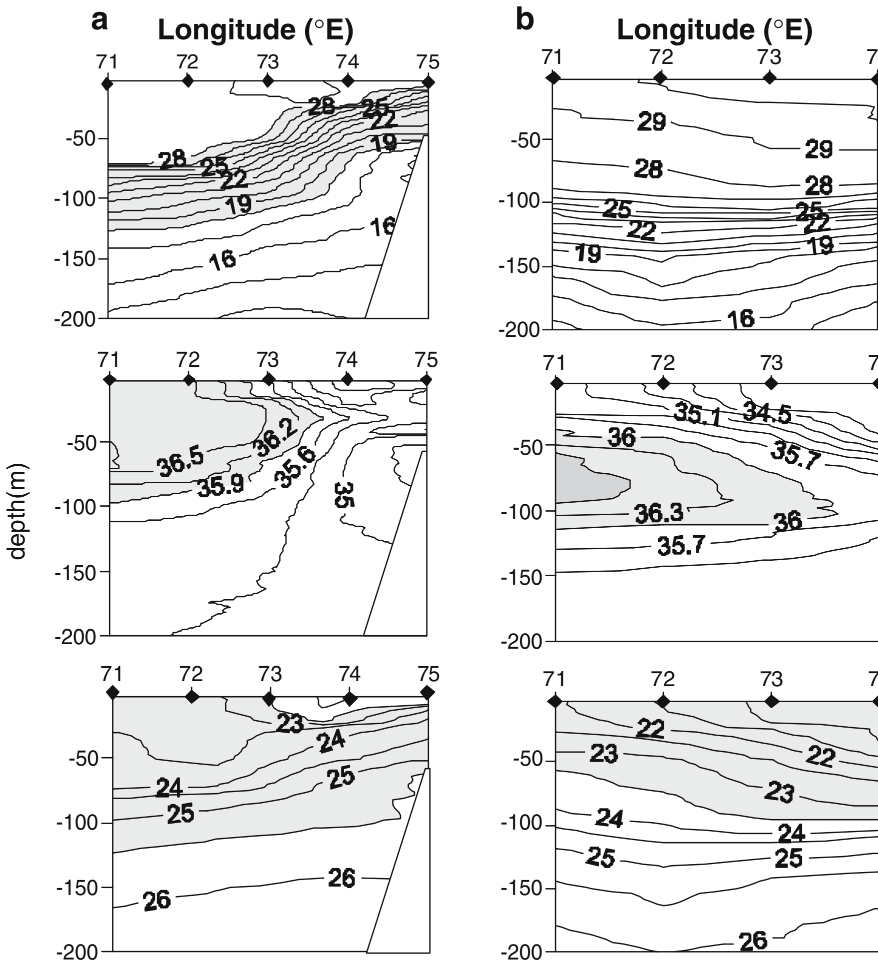

Fig. 5 Vertical distribution of temperature (°C), salinity and density (σ_t) along 11.5° N during **a** later phase of Southwest monsoon and **b** spring intermonsoon. Shaded profiles represent upslope/downslope in temperature and density section, intrusion of high salinity water in the salinity section

salinity (from 34.4 rising to 36.4), in which the salinity maximum due to the Arabian Sea High Salinity Water (ASHSW) was homogenous with low saline waters in the near shore as well as offshore area. The other sections (II to IV) showed considerable horizontal gradients in surface salinity between shelf stations and offshore stations. A tongue-like distribution indicating intrusion of high saline water towards shelf extending vertically between 60 m and 100 m, from the open ocean was noticed along section III. In general, the ASHSW separates the surface and intermediate water.

Upsloping of pycnocline at the nearest coastal station of 8°N section is a signature of upwelling. All other sections displayed down sloping of sigma-t in the upper 100 m. Below 100 m, uplifting of sigma-t values resemble the temperature profiles. The maximum sigma-t gradients were observed at 40 to 80 m depth (1 to 1.7 kg/m^3) in transects IV and V, while in transects I–III the maximal vertical density gradient (1.2 to 2 kg/m^3) was between about 100 and 130 m and the upper layer was highly stable in the area.

From the vertical profile of DO and nutrients, we found that the upper 0–80 m shelf waters were oligotrophic with very low nutrients (NO3 < 1 μm and PO4 < 0.5 μm) and were saturated with oxygen (Fig. 8b). Chl-*a* values were relatively low compared with those in the later phase of summer monsoon. The surface chl-*a* ranged from 0.09 to 0.51 mg m^{-3} (av. 0.2 mg m^{-3}) and column chlorophyll ranged from 4.6 to 25.7 mg m^{-2} (av.15.3 mg m^{-2}) in the near-shore stations (Fig. 9).

The dynamic topography of the surface and 50 m demonstrates the anticyclonic flow associated with

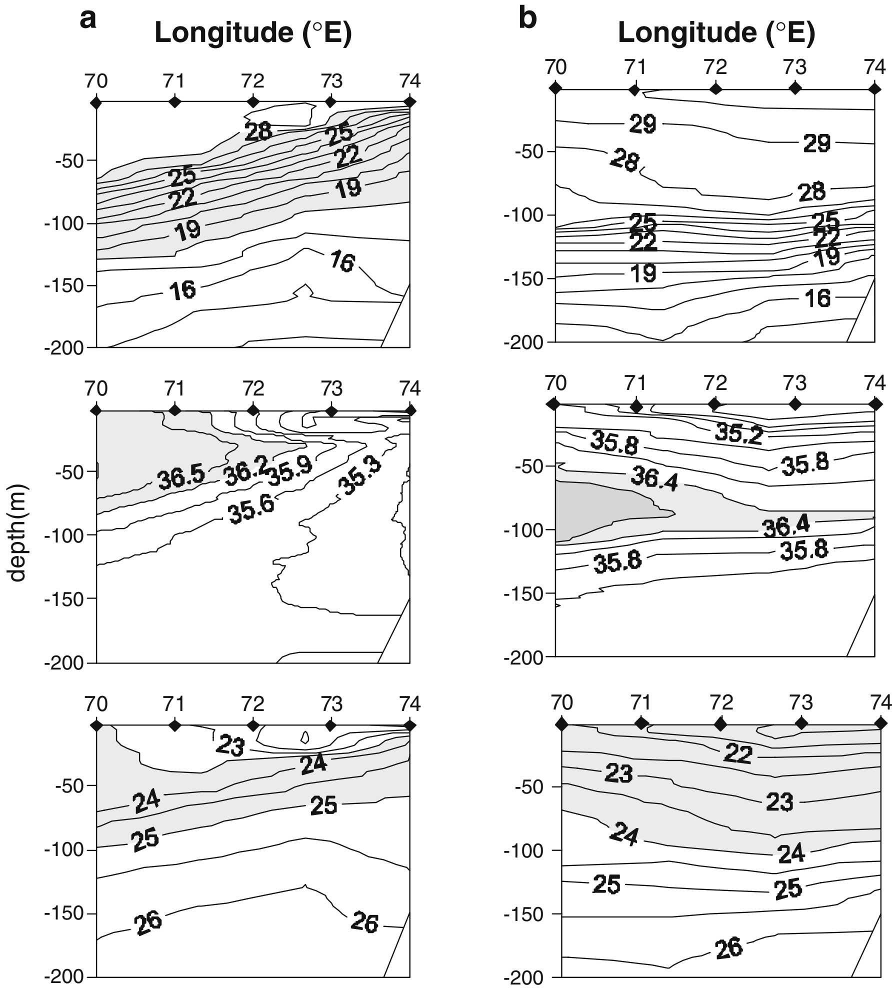

Fig. 6 Vertical distribution of temperature (°C), salinity and density (σ_t) along 13°N during **a** later phase of Southwest monsoon and **b** spring intermonsoon. *Shaded profiles* represent upslope/downslope in temperature and density section, intrusion of high salinity water in the salinity section

Lakshadweep High (LH) with an equator-ward current along the shelf (Fig. 11). At the 100 db level, the southward current widened on the shelf and the eddy was shifted further offshore. At 200 db, the same circulation pattern was observed but with reduced strength. Eddy features were found along 8°N section at all dynamic height surfaces.

Discussion

The interpretation of thermo-haline and density structure gives a general idea of the hydrography of the study area. During the SWM (September) the alongshore component of the winds towards the equator was the driving force of the upwelling system as found by Shetye et al. (1990). In the hydrography section, the shallowing of isoclines of temperature and density clearly indicates the presence of coastal upwelling along all the sections, even at the last phase of the southwest monsoon. The clearest indication of coastal upwelling is the upward slope of isotherms and associated isopycnals towards the coast (Bearman 1989). The up sloping of isotherms and isopycnals represented southward flowing current. Another feature noted was deepening of isotherms and isopycnals below the bottom layer of shallowing of isotherms. This subsurface poleward current appears to be associated with upwelling. The current structure at different levels (Fig. 10) displayed that WICC flows equator ward, deepens to 50 m in the shelf area and below that reversal of currents was noted in the

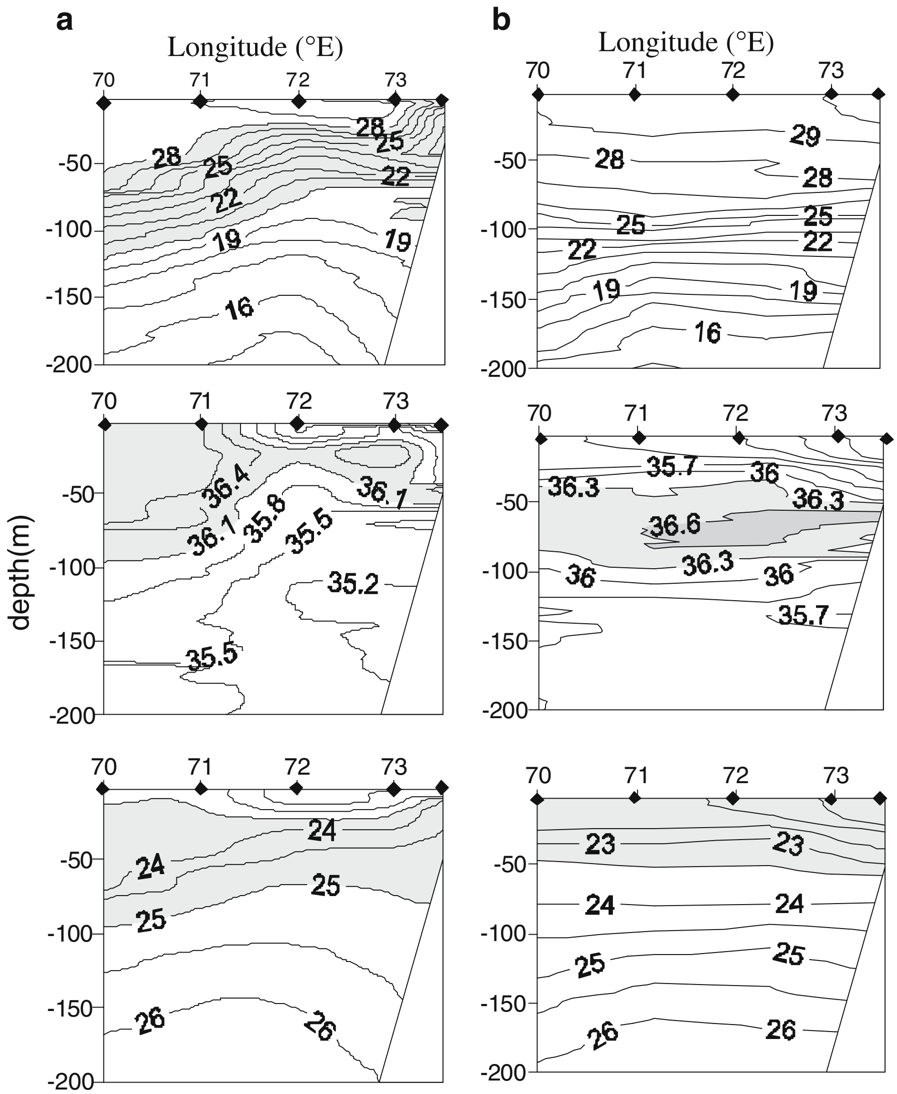

Fig. 7 Vertical distribution of temperature (°C), salinity and density (σ_t) along 15°N during **a** later phase of Southwest monsoon and **b** spring intermonsoon. Shaded profiles represent upslope/downslope in temperature and density section, intrusion of high salinity water in the salinity section

subsurface layer. These results do not show any significant change from the observation of Shetye et al. (1990) that upwelling or the upward slope of the density surface towards the coast was consistent with the southerly current. The associated water properties are illustrated in the vertical section of the parameters such as temperature, salinity and sigma-t. The southeastward WICC played a major role in bringing the high saline water from the north as observed in the off shelf waters of the study region. The low saline water observed in the shelf area due to extensive runoff from rivers and backwaters (Darbyshire 1967) and the strong equator ward currents along the shelf defuse the intrusion of high saline water to the shelf.

Figure 10 clearly illustrates that the reversal of current direction at subsurface, and undercurrent are considered as associated features of the upwelling system (Muraleedharan et al. 1995). The under current is intensified more at 100 db, than at 50 db level which also supports the hydrographic observations. Moreover the spreading of undercurrent is observed at the southern transect rather than at the northern transects and it is found that the under current is closely related to shelf width along the study area. Antony (1990) explains that based on the shelf width,

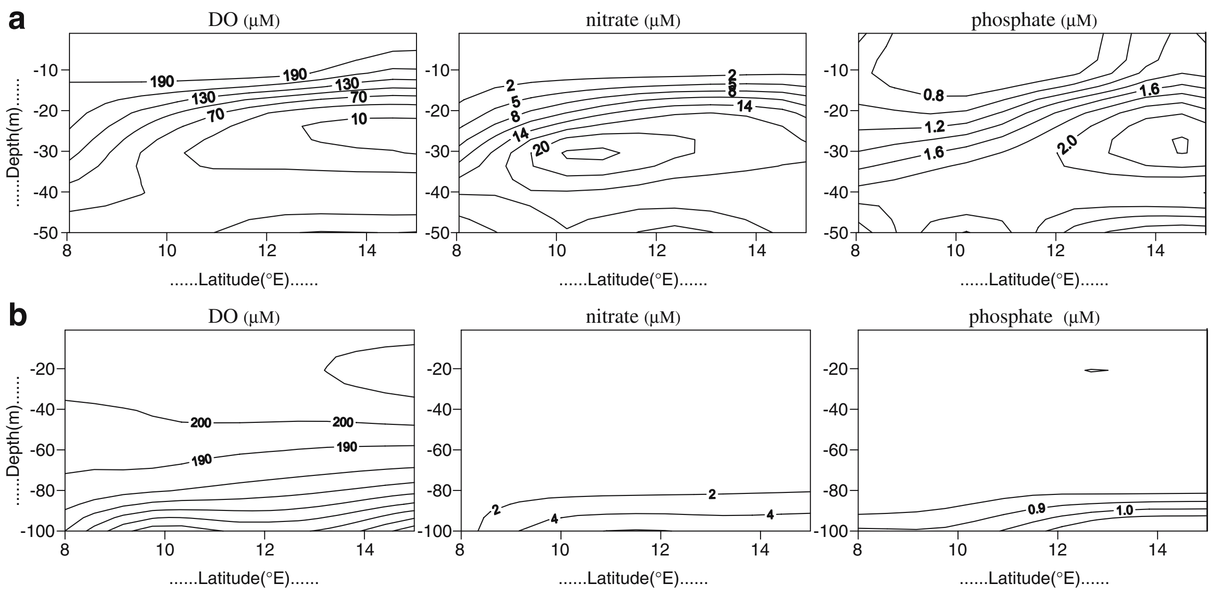

Fig. 8 Distribution of dissolved oxygen (μM), and phosphate (μM) along the continental shelf during **a** later phase of SW monsoon and **b** spring intermonsoon

the shelf induces a baroclinic component towards the equator. The hydrographic section of undercurrent characterized by temperature (19–14°C), salinity (35–35.3) and density (25–26.2) indicates intrusion of low saline equator water associated with the subsurface northward currents.

Another feature associated with upwelling system is a thermal front parallel to the coast, identified from the hydrographic observation (Fig. 12). The coastal thermal front, observed between 11 and 15°N, from the horizontal temperature field of 20 to 50 m depths, doesn't show any signature at the surface and below 75 m depths. The thermal front is found stronger at shelf waters off 11.5 and 13°N transects. The front is observed to be closer to the shore in the northern part than in the southern section giving the impression that the front is moving away from the coast indicating the retarding stages of upwelling.

The local temperature anomalies (LTA) show signature of upwelling in the north and almost retarding stage of upwelling in the southern-most section. LTA was recorded at 0.5, 0.05, 0.3, 0.6 and 2.4°C at Sections I to

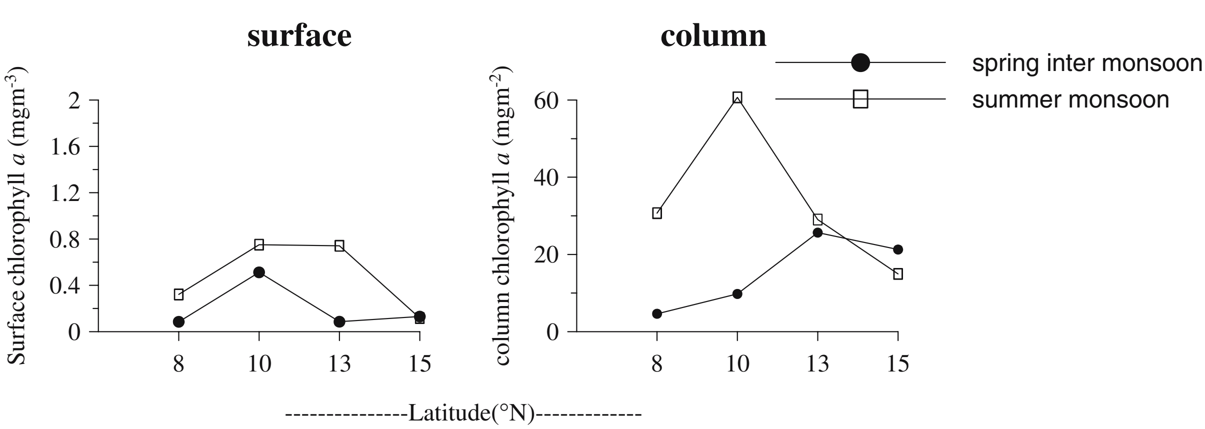

Fig. 9 Distribution of surface and column Chlorophyll *a* on the near shore stations during the later phase of SW monsoon and spring intermonsoon

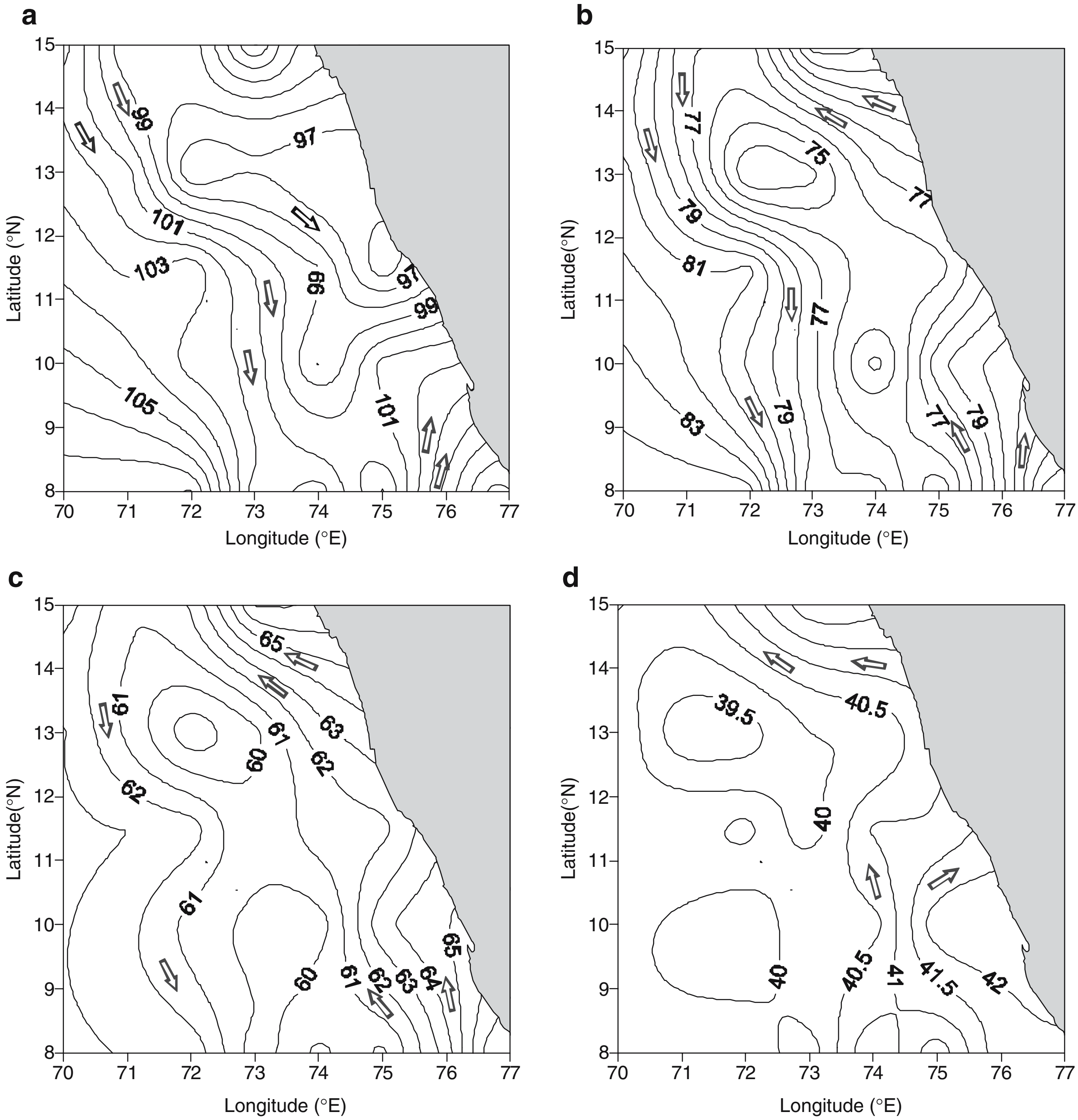

Fig. 10 Dynamic topography (dyn. cm) of **a** sea surface, **b** 50 db, **c** 100 db, and **d** 200 db relative to 500 db during later phase of SW monsoon. *Arrows* indicate the direction of the flow

V (Fig. 13) respectively. This gives an impression that upwelling is intense on the northern side compared to the southern side. Another index, Ekman transport, also shows an increase in magnitude (1,350 and 1,200 kg m^{-1} s^{-1}) at 11.5 and 15°N. It was 200, 400, 500 kg m^{-1} s^{-1} respectively at Section I, II and IV. The relation between these two indices showed good correlation between upwelling and local winds at 15°N whereas at 11.5°N, poor correlation between upwelling and local winds suggests the influence of remote forcing (McCreary et al. 1993; Shankar et al. 2002; Shenoi et al. 2004). At 8°N and 10°N, weak LTA and mass transport represents the retarding stages of upwelling at the southern sections.

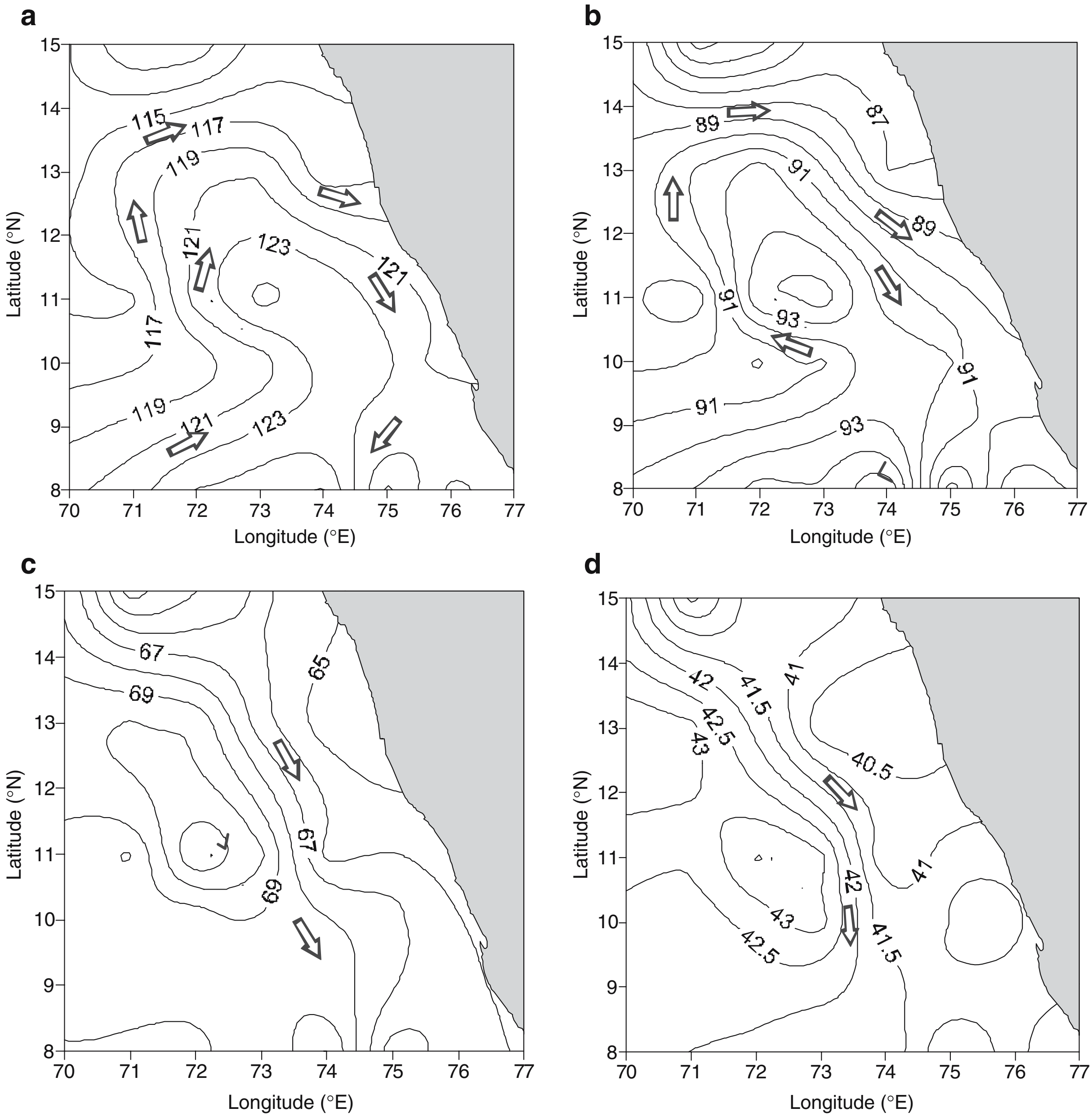

Fig. 11 Dynamic topography (dyn. cm) of **a** sea surface, **b** 50 db, **c** 100 db, and **d** 200 db relative to 500 db during spring intermonsoon. *Arrows* indicate the direction of the flow

Upwelling is generally related to wind-induced Ekman transport thereby the cold and nutrient rich bottom and subsurface waters enter the photic zone resulting in enhanced primary production (Mann and Lazier 1996). Even though the upsloping of isolines of temperature, density and nutrients indicates upwelling signatures are strong in northern part, Chlorophyll and primary productivity (not shown) were observed high off Kochi (10°N) during the period of observation. The climatology of chlorophyll derived from Sea-WiFS (Fig. 14) for the month of September follows the same pattern as observed in

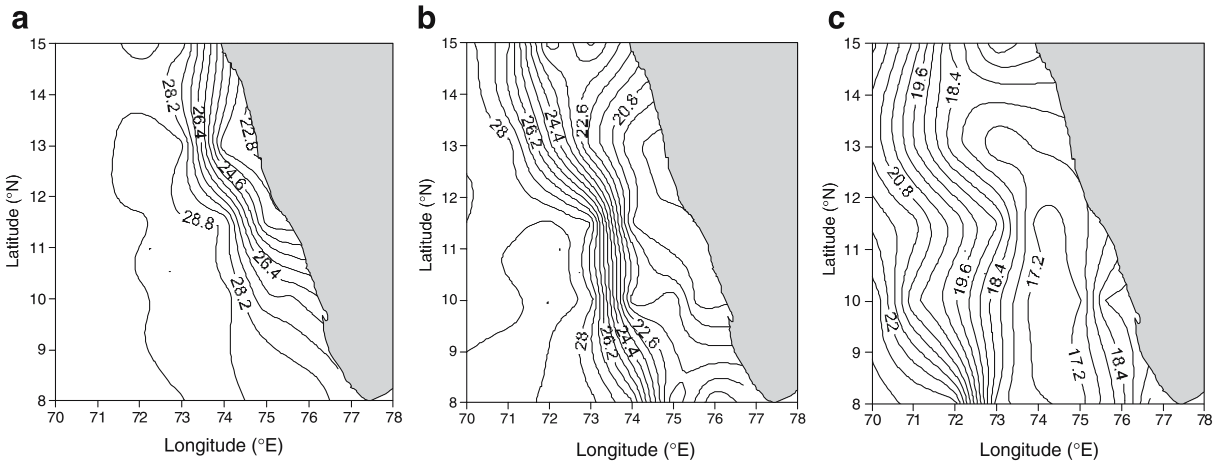

Fig. 12 Thermal structure at different depths **a** 20 m, **b** 50 m, **c** 100 m during the later phase of SW monsoon

the insitu data. Climatology of surface chlorophyll showed the highest concentration off Kochi, with the next high off Mangalore (13°N). During October, the high shifted to off Mangalore and off Goa (15°N). Small (1973) suggested that greater productivity could be observed during relaxation of upwelling than during strong upwelling. Huntsman and Barber (1977) have shown that the most productive conditions off northwest Africa resulted from weak or moderate upwelling favorable winds rather than from strong winds. The lower intensity of upwelling allows the phytoplankton cells longer residence in optimal light near the surface for more effective utilization of the available nutrients and as a result the transient state of rapid relaxation of upwelling forms the most productive condition (Small and Menzies 1981). In conclusion, both the in situ and satellite observations strongly suggest the existence of lag phase between the strong upwelling and intense production.

The hydrography of the SEAS during SIM is associated with high SST (>29°C), low saline water (33.8 to 35.2) in the inner and outer shelf. The water was oligotrophic in nature with low nutrients (NO3< 1 µm and PO4<0.5 µm) and was saturated with oxygen (Fig. 8b). Chl-*a* values were also found relatively low compared to those in September, which also represents SIM characterization. The thermocline base was found deeper at near shore areas than in September. A layer of weak temperature gradient existed between the upper isotherms and top of the thermocline due to winter deepening of thermocline in March, supporting Varkey et al. (1979).

Sea surface salinity distribution in March clearly suggests low saline Bay of Bengal water associated with northerly current in the SEAS (Darbyshire 1967; Shetye et al. 1991; Prasanna Kumar et al. 2004). The Poleward WICC brings the low saline waters along the west coast of India during winter monsoon and when Lakshadweep High (LH) develops at the later phase of the season, the clockwise circulation brings back the low saline water to the southern part of the study area. The Winter Monsoon Current (WMC) branches off on the west of the LH, which lowers the salinity of the offshore stations at 8°N. This is the reason for existence of homogeneous saline water (34.2 to 34.6) in the shelf and offshore waters of the southernmost transect.

During SIM, the circulation pattern (Fig. 11) was clockwise around high locations off 11°N and north of 13°N it was poleward. A clockwise circulation was found extending to 50-db level propagating offshore. During the winter monsoon, westward WMC carries the poleward WICC along the west coast of India. These currents are associated with down welling Kelvin waves which turn around Sri Lanka to propagate poleward along the Indian west coast, radiating westward propagating Rossby waves and leading to the formation of the LH in the SEAS (Bruce et al. 1994, 1998; Shankar and Shetye 1997). As the LH extends and propagates westward, the high sea level pinches off the coast and clockwise

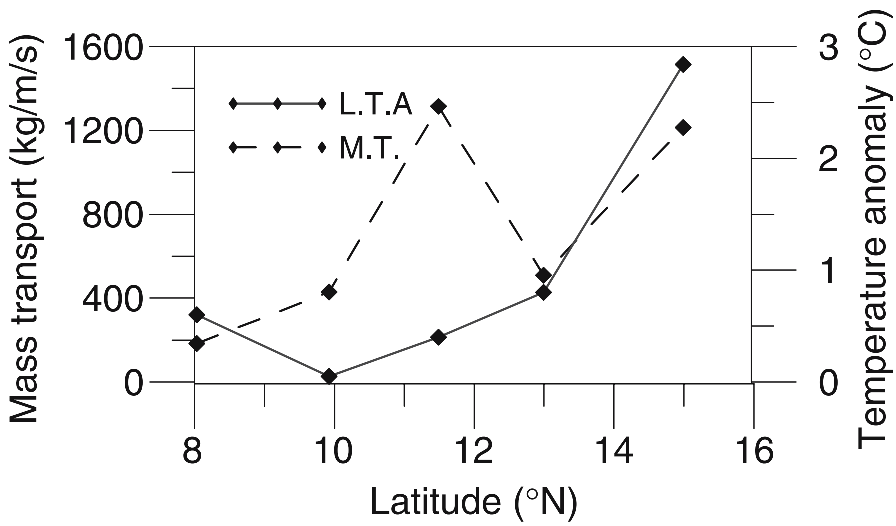

Fig. 13 Latitudinal variation of LTA and M.T. during later phase of SW monsoon

circulation develops around it with a pole ward flow on the western side and an equator-ward flow on the eastern side (Shenoi et al. 2005). At 100 and 200 db level the presence of weak southward undercurrent was observed.

The T-S scatter plot (Fig. 15) for all the CTD profiles has given an insight into the water mass structure of the study region in the upper 1,000 m depth. Three water masses such as Arabian Sea High Salinity Water (ASHSW), Persian Gulf Water (PGW) and Red sea Water (RSW) were identified based on salinity maxima and σ_t structure following the classification of Rochford (1964) during late summer monsoon and spring inter monsoon. Thermohaline characteristics of these water masses are given in Table 1.

ASHSW was traced in the shelf waters of northern section and outer shelf of southern most section during

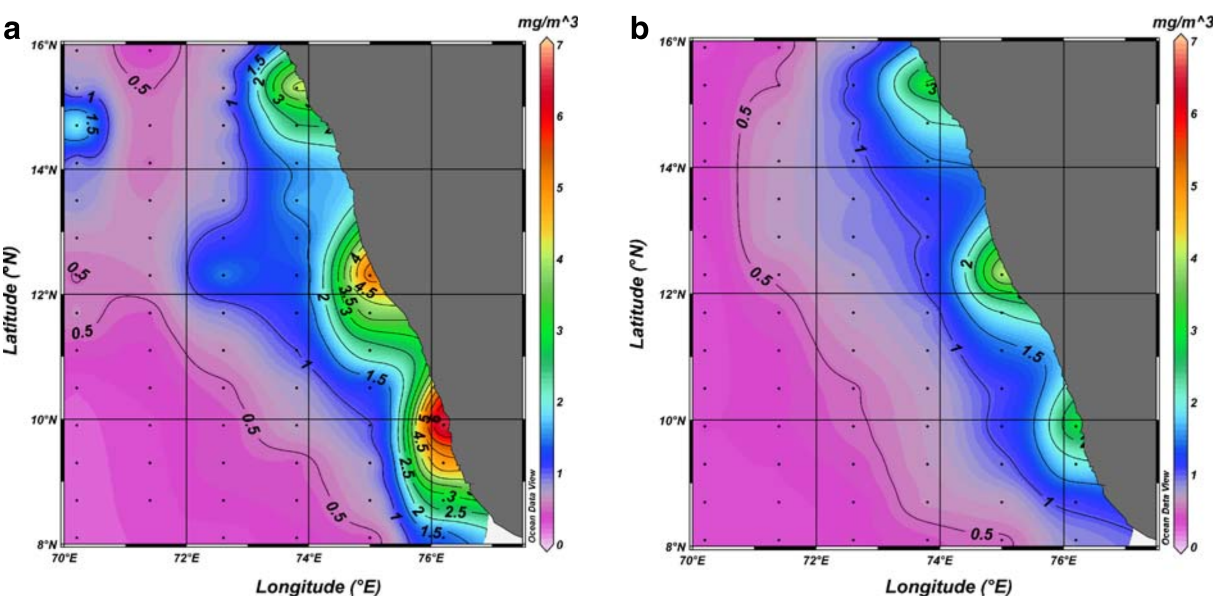

Fig. 14 Climatology of chlorophyll-*a* derived from Sea-WiFs for **a** September and **b** October month

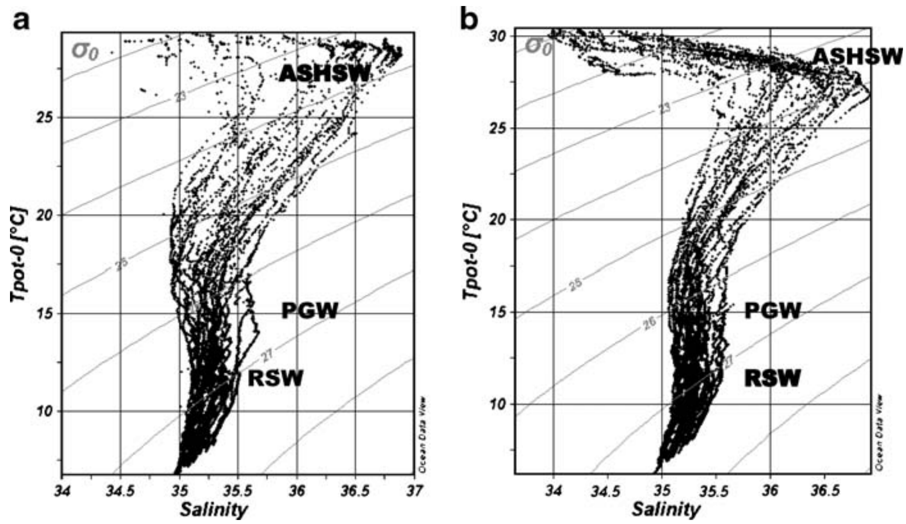

Fig. 15 Temperature-salinity (*TS*) diagram for all CTD profiles collected during the hydrographic survey **a** later phase of SW monsoon and **b** spring intermonsoon

both the study periods. The depth of occurrence of ASHSW, as inferred from salinity maxima, varies between surface and 80 m and σ_t found varied from 23.0 to 24.5. During Spring Inter monsoon, it was found at deeper depth (40 to 100 m), because of the presence of low saline water in the upper surface of the shelf and offshore waters. Also, the concentration of ASHSW was very much reduced at southern section during March compared to the later phase of SWM. According to Prasanna Kumar and Prasad (1999), after formation in the northern Arabian Sea during the winter monsoon, ASHSW spreads predominantly southwards along the eastern boundary during the summer monsoon.

Persian Gulf Water was present at depths between 200 and 300 m within the σ_t range of 26.4–26.8 during September and 26.2–26.6 sigma-t surface during March. PGW was dominant in the northern part of the study area and it was less observed in the south (Ramesh Babu et al. 1980; Varadachari et al. 1974). The signals of PGW were weak in the study area during September. After intense mixing in the Strait of Hormuz, the warm (17°C) and high salinity (>36.2) PGW enters the Arabian sea to form a subsurface salinity extreme between 200 and 300 m and the value decreased to cold (12 to 15°C). Low salinity (35.1–35.5) along the west coast of India is maintained by lateral mixing with low salinity Bay of Bengal water during winter (Prasad et al. 2001). The deepening of the PGW depth during SIM is associated with monsoon changes in the Arabian Sea circulation.

Presence of Red Sea Water in the study area was noticed in the 27.0 to 27.3 σ_t surfaces at 450–600 and 500–750 m depths respectively during SW monsoon and inter monsoon. In March, it was deeper than in September, which may be associated with current patterns. The Red Sea Water formed at Red Sea basin, enters the Gulf of Aden through the Bab el Mandeb,

Table 1 Thermohaline characteristics of different water masses in the south-eastern Arabian Sea during later phase of southwest monsoon and spring intermonsoon

Month	Temp (°C)	Salinity	σ_t (kg/m³)	Depth (m)
Arabian Sea High Saline Water (ASHSW)				
September	29–24	36.2–36.8	23.0–24.5	0–80
March	28–25	36.2–36.8	23.0–24.5	40–100
Persian Gulf Water (PGW)				
September	12–15	35.1–35.5	26.4–26.8	230–260
March	13–16	35.1–35.5	26.2–26.6	230–300
Red Sea Water (RSW)				
September	10–12	35.1–35.5	27.0–27.2	450–600
March	10–13	35.2–35.6	27.0–27.3	500–750

further spreads into the Arabian Sea leading to a zonal decrease in salinity towards south with depth changing from 450 to 650 m. In general, the signal of ASHSW, PGW and RSW decreased towards southern sections, as is well known.

Conclusion

The southeastern Arabian Sea showed seasonal variability in the hydrographic field and current pattern during SIM (March 2004) and later phase of SWM (September 2003). Signature of upwelling was observed in the later phase of SWM along the near shore stations, prominent in the northern section and retarding in the south. The biological impact of upwelling records maximum productivity during the observation period at the southern transects (10°N lat) even though prominent upwelling was found in the north. The influence of high saline water during September and low saline water during inter monsoon was observed in the surface layers of SEAS. During September, the current pattern was the continuation of monsoon circulation, with Equator ward WICC at surface and pole ward undercurrent at subsurface. During spring inter monsoon, the flow was found to be linked with LH in the south, and north of 13°N, WICC flows pole-ward.

Acknowledgements We thank Dr. S.R. Shetye, Director, National Institute of Oceanography, India for the facilities provided to carry out this study. We also express our gratitude to Ministry of Earth Sciences for financial support of the work and to the Director, CMLRE (MOES), Kochi, India for providing FORV Sagar Sampada for onboard data collection. This is NIO contribution 4212.

References

Antony, M. K. (1990). Northward undercurrent along West coast of India during upwelling – some inferences. *Indian Journal of Marine Sciences, 19*, 95–105.

Banse, K. (1959). On upwelling and bottom trawling off the Southwest coast of India. *Journal of the Marine Biological Association of India, 1*, 33–49.

Bearman, G. (1989). Coastal upwelling in eastern boundary currents. In Bearman (Ed.), *Ocean circulation* (p. 118). Oxford: Pergamon Press.

Bruce, J. G., Johnson, D. R., & Kindle, J. C. (1994). Evidence for eddy formation in the Eastern Arabian Sea during the northeast monsoon. *Journal of Geophysical Research, 99*, 7651–7664.

Bruce, J. G., Kindle, J. C., Kantha, L. H., Kerling, J. L., & Bailey, J. F. (1998). Recent observations and modeling in the Arabian Sea Laccadive high region. *Journal of Geophysical Research, 103*, 7593–7600.

Darbyshire, M. (1967). The surface waters off the coast of Kerala, Southwest India. *Deep Sea Research, 14*, 295–320.

Huntsman, S. A., & Barber, R. T. (1977). Primary production of North West Africa: The relationship with wind and nutrient conditions. *Deep Sea Research, 24*, 25–34.

Jayaraman, R., Ramamirtham, C. P., Sundararamam, K. V., & Aravindakshan Nair, C. P. (1960). Hydrography of the Laccadive offshore waters. *Journal of the Marine Biological Association of India, 2*(1), 24–34.

Johannessen, O. M., Subbaraju, G., & Blindhejm, J. (1981). Seasonal variations of the oceanographic conditions off the Southwest coast of India during 1971–1975. *Fiskeridirektoratets Skrifter, Serie Havundersøkelser, 18*, 247–261.

Joseph, P. V. (1990). Warm pool over the Indian Ocean and monsoon onset. *Tropical Ocean Newsletter, 53*, 1–5.

Joseph, W. L., & Kantha, L. H. (2000). Results from a numerical model of the Northern Indian Ocean: Circulation in the South Arabian Sea. *Journal of Marine Systems, 24*, 97–117.

Mann, K. H., & Lazier, J. R. N. (1996). *Dynamics of marine ecosystem: Biological–physical interactions in the ocean* (2nd ed.). Cambridge, MA, U.S.A.: Blackwell Science.

McCreary, J. P., Kundu, P. K., & Molinari, R. L. (1993). A numerical investigations of the dynamics, thermodynamics and mixed-layer processes in the Indian Ocean. *Progress in Oceanography, 31*, 181–244.

Muraleedharan, P. M., & Prasanna Kumar, S. (1996). Arabian Sea upwelling – a comparison between coastal and open ocean regions. *Current Science, 71*, 824–846.

Muraleedharan, P. M., Ramesh Kumar, M. R., & Gangadhara Rao, L. V. (1995). A note on poleward undercurrent along the Southwest coast of India. *Continental Shelf Research, 15*, 165–184.

Patil, M. R., & Ramamirtham, C. P. (1963). Hydrography of the Laccadive offshore waters – a study of winter conditions. *Journal of the Marine Biological Association of India, 5*(2), 159–169.

Prasad, T. G., Ikeda, M., & Prasanna Kumar, S. (2001). Seasonal spreading of the Persian Gulf Water mass in the Arabian Sea. *Journal of Geophysical Research, 106*, 17059–17071.

Prasanna Kumar, S., Jayu, N., Ajoy, K., Shaji, C., Anand, P., Sabu, P., et al. (2004). Intrusion of the Bay of Bengal water into the Arabian Sea during winter monsoon and associated chemical and biological response. *Geophysical Research Letters, 31*, L15304. Retrieved from doi:10.1029/2004GL020247.

Prasanna Kumar, S., & Prasad, T. G. (1999). Formation and spreading of Arabian Sea high-salinity water mass. *Journal of Geophysical Research, 104*, 1455–1464.

Prell, W. L., & Streeter, H. F. (1982). Temporal and spatial patterns of monsoonal upwelling along Arabia: A modern analogue for the interpretation of quaternary SST anomalies. *Journal of Marine Research, 40*, 143–155.

Ramamirtham, C. P., & Jayaraman, R. (1960). Hydrographical features of the continental shelf waters off Cochin during the years 1958 & 1959. *Journal of the Marine Biological Association of India, 2*(2), 199–207.

Ramesh Babu, V., Varkey, M. J., Kesava Das, V., & Gouveia, A. D. (1980). Water masses and general hydrography along the West coast of India during early March. *Indian Journal of Marine Sciences, 9*, 82–89.

Rochford, D. J. (1964). Salinity maxima in the upper 1000 meters of the North Indian Ocean. *Australian Journal of Marine and Freshwater Research, 15*, 1–24.

Sastry, A. A., & Myrland, P. (1959). Distribution of temperature, salinity and density in the Arabian Sea along the South Malabar Coast (South India) during the post-monsoon season. *Indian Journal of Fisheries, 6*(2), 223–255.

Shankar, D., & Shetye, S. R. (1997). On the dynamics of the Lakshadweep high low in the Southeastern Arabian Sea. *Journal of Geophysical Research, 102*, 12551–12562.

Shankar, D., Vinayachandran, P. N., & Unnikrishnan, A. S. (2002). The monsoon currents in the North Indian Ocean. *Progress in Oceanography, 52*, 63–120.

Sharma, G. S. (1978). Upwelling off the Southwest coast of India. *Indian Journal of Marine Sciences, 7*, 209–218.

Shenoi, S. S. C., Shankar, D., Michael, G. S., Kurian, J., Varma, K. K., Ramesh Kumar, M. R., et al. (2005). Hydrography and water masses in the Southeastern Arabian Sea during March–June 2003. *Journal of Earth System Science, 114*(5), 475–491.

Shenoi, S. S. C., Shankar, D., & Shetye, S. R. (1999). On the sea surface temperature high in the Lakshadweep Sea before the onset of the southwest monsoon. *Journal of Geophysical Research, 104*, 15703–15712.

Shenoi, S. S. C., Shankar, D., & Shetye, S. R. (2004). Remote forcing annihilates barrier layer in Southeastern Arabian Sea. *Geophysical Research Letters, 31*, L15307. Retrieved from doi:10.1029/2003GL019270.

Shetye, S. R., Gouveia, A. D., Shenoi, S. S. C., Sundar, D., Michael, G. S., Almedia, A. M., et al. (1990). Hydrography and circulation off the West coast of India during the southwest monsoon 1987. *Journal of Marine Research, 48*, 359–378.

Shetye, S. R., Gouveia, A. D., Shenoi, S. S. C., Sundar, D., Michael, G. S., Almeida, A. M., et al. (1991). The coastal current off Western India during the northeast monsoon. *Deep Sea Research, 38*, 1517–1529.

Shetye, S. R., Shenoi, S. S. C., Antony, M. K., & Krishna Kumar, V. (1985). Monthly mean wind stress along the coast of the North Indian Ocean. *Proceedings of Indian Academy of Sciences (Earth and Planetary Sciences), 94*(2), 129–137.

Small, L. F. (1973). Chlorophyll and optical properties in CUE-I upwelling region. In N. K. Moores & J. S. Allen (Eds.), *Final report of the coastal upwelling, ecosystem analysis, summer 1973, theoretical workshop*. Washington: NSF/IOOE Office.

Small, L. F., & Menzies, D. W. (1981). Patterns of primary productivity and biomass in a coastal upwelling region. *Deep Sea Research, 28A*, 123–149.

Strickland, J. D. H., & Parsons, T. R. (1972). A practical handbook of seawater analysis. In *Fisheries Research Board of Canada Bulletin 177* (2nd ed., p. 310). Ottawa: Queen's Printer

Varadachari, V. V. R., Murty, C. S., & Sankaranarayanan, V. N. (1974). Physical characteristics of waters & water masses off the West coast of India during late spring. *Indian Journal of Marine Sciences, 3*, 1–3.

Varkey, M. J., Kesava Das, V., & Rama Raju, D. V. (1979). Physical characteristics of the Laccadive sea (Lakshadweep). *Indian Journal of Marine Sciences, 8*, 203–210.

Wyrtki, K. (1971). *Oceanographic atlas of the International Indian Ocean expedition*. Washington D.C.: National Science Foundation, U.S. Government of Printing Office.